의학박사 학위논문

Identification of *Plasmodium falciparum*-specific kinase inhibitors: candidates for a potent antimalarial drug

항말라리아제 후보 물질로서 열원충 키나아제에 특이적인 저해제의 발굴

2013 년 2 월

서울대학교 대학원

의학과 기생충학

구 민 제

A thesis of the Degree of Doctor of Philosophy

항말라리아제 후보 물질로서 열원충 키나아제에 특이적인 저해제의 발굴

Identification of *Plasmodium falciparum*-specific kinase inhibitors: candidates for a potent antimalarial drug

February, 2013

The Department of Parasitology and Tropical Medicine,

Seoul National University

College of Medicine

Min-Je Ku

Identification of *Plasmodium falciparum*-specific kinase inhibitors: candidates for a potent antimalarial drug

by Min-Je Ku

(Supervised by Prof. Min-Ho Choi)

A thesis submitted to the Department of Medicine in partial fulfillment of the requirements for the Degree of Doctor of Philosophy in Parasitology and Tropical Medicine at Seoul National University College of Medicine

December, 2012

Approved by Thesis Committee

Professor _____ **Chairman**

Professor _____ **Vice chairman**

Professor _____

Professor _____

Professor _____

Abstract

Identification of *Plasmodium falciparum*-specific kinase inhibitors: candidates for a potent antimalarial drug

Min-Je Ku
The Dept of Parasitology and Tropical Medicine
The Graduate School
Seoul National University

Background: Malaria is a disease caused by protozoan parasites of the genus *Plasmodium* and results in almost a million deaths annually. Currently, the resistance to the available anti-malarial drugs is the biggest obstacle to control the disease. Thus, there is an urgent need for developing a new drug having different parasitic targets. *Plasmodium* kinases are emerging attractive targets for a novel antimalarial drug because they play essential roles for the parasites while they are very different from the mammalian kinases structurally and even functionally. Therefore, in this study, I looked for the small molecules that can inhibit kinases of malaria parasites, which can be developed into a novel antimalarial drug in the future.

Methods: In order to find *Plasmodium falciparum*-specific kinase inhibitors, 4000

kinase-directed inhibitors were screened using a SYBR green I assay against wild type (3D7) and drug resistant strains (Dd2) of *P. falciparum*. Some of the hits were tested using fluorescence-based thermal shift assay (FSA) and kinase assay to find their kinase targets. They were also tested in a related apicomplexan parasite, *Toxoplasma gondii* to prove the suggested target. *In silico* molecular docking analysis was performed to propose the possible binding modes between the small molecules and the target protein.

Results: The primary screening resulted in the identification of 23 compounds that are highly active for both 3D7 and Dd2 strains but have low toxicity profiles in human cell lines. *Plasmodium falciparum* calcium-dependent protein kinase 1 (PfCDPK1) was found to be a possible target for three compounds using the enzyme-based FTA and kinase assay. The three compounds inhibited invasion of *T. gondii* into U2OS cells, supporting the target of these particular compounds is CDPK1. Molecular docking analysis suggests the three compounds might have ATP-competitive but not ATP-mimetic mode of binding with the enzyme, which is different from conventional kinase inhibitors.

Conclusions: The present study will contribute to develop a new antimalarial drug targeting *Plasmodium* kinases in the future. Particularly, the three compounds targeting PfCDPK1 will be a good start to design a novel PfCDPK1 inhibitor for an antimalarial drug.

Keywords: malaria, *Plasmodium falciparum*, antimalarial drug, protein kinase, CDPK1, kinase inhibitor

Student number: 2009-31098

Contents

List of Figures

List of Table

Introduction

Malaria is one of the most devastating diseases, which is responsible for one million deaths every year in worldwide [1,2]. Most of the deaths are the African young children under 5 years of age and approximately half of the world's population is at risk of malaria. Malaria is caused by protozoan parasites of the genus *Plasmodium,* five species of which are known to infect humans, *P. falciparum, P. vivax, P. malariae, P. ovale, and P. knowlesi*. Of these five, *P. falciparum* is responsible for the most severe forms of malaria such as cerebral malaria [3] and pregnancy-associated malaria [4]. *P. falciparum* have several morphological changes during their complex life cycle (Fig. 1). Upon infection by an infected *Anopheles* mosquito, sporozoites are injected to the host, rapidly accessing to the liver and invade hepatocytes, where asymptomatic asexual multiplication (exoerythrocytic schizogony) occurs. This leads to the production of several thousand merozoites that are released in the blood stream and invade erythrocytes to proceed with erythrocytic schizogony causing severe pathologic symptoms. During this phase, the parasite in the erythrocyte undergoes dramatic changes in their forms that include ring, trophozoite, and schizont stages. Some of the merozoites, after the invasion of erythrocytes, arrest their cell cycle and differentiate into male or female gametocytes, leaving behind until another mosquito takes them for generation of infective sporozoites produced after sexual fertilization inside the mosquito. When

this mosquito finds another human host, transmission starts. This complex life cycle having several stage-conversion steps is highly and sophisticatedly controlled by the parasite in response to cellular stimulation [5,6].

Antimalarial chemotherapy remains the only option for the treatment of patients infected by the malaria parasite due to the lack of suitable vaccines. Currently available antimalarials are devided into four groups depending on the mode of actions and the chemical structures of the compounds: quinolines, antifolates, atovaquone/proguanil, and artemisinins. Quinolines are originated from quinine - the active ingredient of the *Cinchona* bark – that has quinoline ring in the core structure. Most of the known quinoline antimalarials are the derivatives of quinoline ring such as chloroquine (CQ), amodiaquine (ADQ), premaquine (PQ) and mefloquine (MQ). All of these compounds (except PQ used for combating *P. vivax* infections) are thought to share the target: formation of the parasite-specific substance hemozoin that is polymerized to detoxify heme released when the hemoglobin is digested by the parasite. CQ and related drugs prevents from polymerization of hemozoin, thereby, leading to the accumulation toxic heme inside parasites and killing them. Antifolates that include pyrimethamine (PYR) and sulfadoxine (SDX) are the inhibitors of dihydrofolate reductase (DHFR) and dihydroopteroate synthase (DHPS) respectively, the enzymes in the folate pathway which are essential for the parasite. Atovaquone (ATV) interferes with mitochondrial electron transport by inhibiting the movement of the iron-sulfur protein subunit in cytochrome b (CYT b) in Complex III [7]. The structural

differences of the target protein between *Plasmodium* and human made ATV as an antimalarial drug. Today, it is used as chemoprophylaxis and administered in combination with the antifolate, proguanil (PG) under the brand name Malarone™. The last antimalarial group, artemisinins (ART) was originated from the Chinese traditional medicine, qinghaosu (extract from the plant *Artemisia annua*). Its potency as an antimalarial medicine was first reported in 1975 in the *Chinese Medical Journal* by anonymous authors. After that, several derivatives of artemisinins were synthesized such as artemether, arteether and artesunate, which are all metabolized into dihydroartemisinin – the main active component in the body. Although the mechanism of action of ARTs is poorly understood, ARTs in combination with other drugs - known as the artemisinin-combination theraphy (ACT) [8]- are currently being used as the most relevant drug to treat uncomplicated malaria.

Despite the availability of current antimalarial drugs, however, a rapid emergence and spread of parasite strains resistant to these drugs have become the biggest obstacle to control malaria [9]. Such resistance relates to the genetic mutation in the target of the drugs. For examples, *pfcrt* that encodes for choloroquine resistance transporter (PfCRT) has been reported as the key gene for CQ-resistant parasites [10]. CQ-sensitive parasites uptake CQ into food vacuole – the site of CQ action – by PfCRT that is located in the membrane of food vacuole. But, in the CQ-resistant parasites, this protein is altered to efflux CQ outside vacuole. Antifolates and ATV that have obvious cellular targets have also been demonstrated the association

between the point mutations of the target genes and the resistance: PYR and SDX resistance have been linked to mutations in *dhfr* and *dhps* that encodes for DHFR and DHPS, respectively [11,12]. The treatment of failure of ATV was also found to be linked to the mutations in the *cyt b* gene of the parasite. To worsen the situation, the artemisinins, which have been considered as the last resort after the emerging resistance for all the other antimalarials, started to threaten with showing its resistance recently [13,14,15]. In fact, the resistance for all the available antimalarials has been reported today [16], therefore, we desperately need a new drug that has different targets.

Protein kinases (PKs) in eukaryotic cells have been known to regulate important cellular processes such as transcription, translation, protein synthesis, cell cycle, and apoptosis [17]. Therefore, they have been attractive drug targets for various cancers [18] and other diseases [19]. *Plasmodium* PKs are not an exception; after the sequence of *Plasmodium* kinome was unveiled [20], experimental evidences that *Plasmodium* PKs are important to trigger life-stage conversions [21] and their involvement in parasite replication [22] as well as parasite-specific processes such as invasion [23] and cytoadherence [24] have rendered *Plasmodium* PKs as potential drug targets. Furthermore, based on the divergences between mammalian and *Plasmodium* PKs: (i) a large proportion of *Plasmodium* kinome is either "orphan" or "semi-orphan" kinases [20], which lack ability to be clustered in well-established eukaryotic PKs (ePKs) or in the latter case, representing atypical roles despite the possibility of clustering to known ePKs, and (ii) even if they belong to

established-ePK family, their catalytic pockets are likely highly different from those of mammalian ePKs [25], finding selective inhibitors of *Plasmodium*-specific kinases has been strongly proposed for a novel antimalarial chemotherapeutic intervention. In addition to these observations, targeted gene disruption studies to know whether these *Plasmodium* PKs are essential for the parasite viability demonstrated that the vast majority of *Plasmodium* PKs are essential enzymes for parasites, thus, being targets for a new antimalarial chemotherapy [26].

In this study, in order to find *P. falciparum*-specific kinase inhibitors that might be a potential candidate for developing an antimalarial drug in the future, kinase-directed inhibitor libraries (4000 compounds) were screened against malaria parasites using *in vitro* parasite-proliferation assay, SYBR Green I assay [27,28]. Given that the library is composed of the compounds that were uniquely designed to target not only a conventional binding site (via a ATP- competitive mode) but also a novel binding site (via an non-ATP-competitive mode) of the enzymes [29], the hit compounds from the screening might be further developed into a novel antimalarial drug. Here, the present study shows 23 compounds that are highly active in *P. falciparum* 3D7 as well as Dd2, the multidrug-resistant strain while they have low toxicity for human cell lines. Out of them, some of the compounds were selected and tested in a panel of recombinant *Plasmodium* kinases to identify their possible targets. *P. falciparum* calcium-dependent-protein kinase 1 (PfCDPK1) was identified as a target for 3 compounds. Furthermore, test of the compounds in a-related parasite, *Toxoplasma gondii* showed they inhibited the parasite's invasion to

U2OS cell, supporting the target of the compounds is PfCDPK1. Molecular docking analysis using the compounds were also performed into known structure of *Plasmodium* CDPK1, where it showed a different binding mode to the enzyme from the mode of ATP. Taken all together, this study demonstrates a novel compounds targeting PfCDPK1, which can be developed into a new anti-malarial drug in the future.

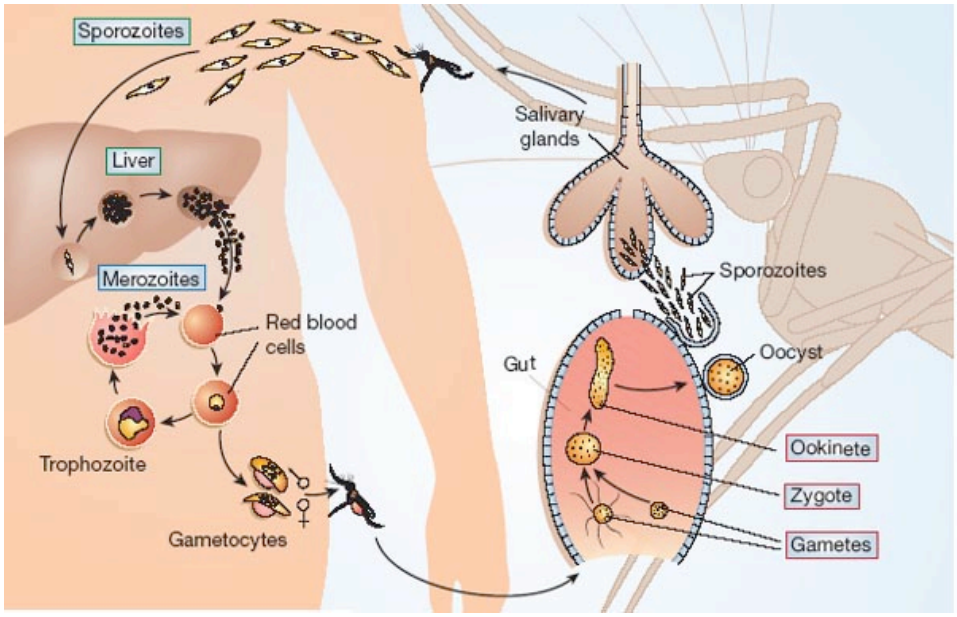

Fig. 1. Life cycle of *Plasmodium*

Three distinct stages of the parasite life cycle. First, the pre-erythrocytic stages include the sporozoites, injected by the mosquito into the skin, and the secondly, liver-stage parasites, which differentiate inside liver cells into merozoites. Third, the erythrocytic (red blood cell) stages primarily comprise merozoites (the figure was extracted from the published paper by Menard *et. al.* (2005) [30]).

Materials and Methods

1. Cultivation of parasites

P. falciparum (3D7 and Dd2 strains) were obtained from MR4 (MRA-102 and MRA-150, respectively) and cultivated in RPMI 1640 media (Welgene, Daegu, Korea) supplemented with *L*-glutamine, 25 mM HEPES, sodium bicarbonate, 0.5% Albumax, 0.1 mM hypoxanthine and 16 μM thymidine in human O^+ erythrocytes. After synchronization with 5% sorbitol, parasites were maintained for at least one complete cycle and late rings or early trophozoites were applied to primary (Biofocus library) screening and secondary hit-confirmation step.

Toxoplasma gondii isolate I was kindly provided by Seoul National University and cultivated in U2OS cells in a DMEM media (Gibco, Life Technologies, NY, USA) supplemented with 10% FBS (Gibco) and 1% Penicilin/Streptomycin (Gibco). $6x10^6$ parasites were added every time in 80-100% confluent U2OS cells to maintain the parasites.

2. The library

The library (BioFocus, Saffron Walden, UK) is a commercial library, which is a collection of 4,000 chemical compounds targeting several kinases [29]. It is uniquely designed to target various kinases through ATP-competitive as well as non ATP-competitive binding mode.

3. Primary screening using SYBR Green I assay

The published SYBR Green I assay protocol [27,28] was modified for high-throughput screening in 384-well plates (Greiner Bio-One, Kremsmuenster, Austria). *P. falciparum* 3D7 and Dd2 cultures (at 0.5% parasitaemia in 2% hct) were incubated for 72 h in 384-well plates together with 10 μM of each compound per well (volume ratio = 45 μL parasite culture : 5 μL compound). For positive and negative controls, final 0.5% DMSO and 400 nM artemisinin (Sigma-aldrich, St. Louis, USA) respectively, were treated in the cultures. After the drug exposure time, 25 μL of lysis buffer containing SYBR Green I (Invitrogen, Life Technologies, NY, USA; 0.3 μL SYBR Green per 1 ml lysis buffer), 30 mM Tris (pH 7.5), 7.5 mM EDTA, 0.012% saponin, 0.12% Triton X-100 were added in each well, which was followed by vigorous mixing using Mixmate (Eppendorf, Hambug, Germany) for 45 sec at 1700 rpm. The plates were incubated for 1 h in dark condition, at room temparature, prior to reading for fluorescence measurements using Victor 3 (PerkinElmer, Messachusetts, USA).

4. Cytotoxicity test for the library

Cytotoxicity test for the whole library was performed at a single concentration point, 10 μM using four different human cell lines: U2OS, HeLa, THP1 and Huh7.5. Cells (5×10^3 cells per well) were seeded in a 384-well plate with 10 μM of each compound and incubated for 72 h at 37°C. After the drug exposure time, resazurin (Sigma) was added (final 10 μM) in each well, which was followed by another

incubation for 12 h at 37°C. The cells were fixed by final 4% paraformaldehyde prior to reading for fluorescence measurement (Victor 3). The cells treated with 0.5 % DMSO and 50 μM chlorpromazine, which were used for positive and negative controls, respectively and the raw data were normalized based on the mean of controls, converting values into 0-100%.

5. Hit confirmation (dose-response curves of the hits)

To assess EC_{50} of compounds, parasite cultures were prepared the same as in primary screening and treated in 384-well plates with serially diluted compounds. The dose ranged from 20 μM to 4.9 nM (4-fold dilution), where each point had duplicates in a different plate. After 72-h drug incubation time, the plates were preceded with SYBR Green I assay as detailed previously. After the assay, the raw data were plotted in Prism 5.0 (Graphpad, San Diego, USA) to achieve dose-response curve of each compound, where EC_{50} of each compound was estimated.

6. Clustering of hit compounds

The compounds (n=109) that were active over 90% for both 3D7 and Dd2 but less toxic for human cells were clustered based on their common scaffolds. As a result, 8 clusters were found to have significance (i.e. each cluster is comprised by more than 5 compounds) and especially, the highly active compounds (n=23) that EC_{50} was under 1 μM fell in the 5 different clusters out of the 8 clusters.

7. Fluorescence-based thermal shift assay

The 9 IPK-coded compounds were tested against individual kinases using a combination of Fluorescence-based thermal Shift Assay (FTA) [28] and standard kinase activity assay (KA). Compounds were screened at a concentration of 5 μM. FTA is performed using around 1 μM of the individual kinase protein and a 5 molar excess of compound. SYPRO Orange (Sigma-aldrich) is used as a fluorescence probe. The temperature was raised 1^{o}C per minute from 25^{o}C to 95^{o}C with fluorescence readings taken every minute.

8. Kinase assay

Kinase assays were performed using the ADP-Glo™ Kinase Assay Kit (Promega, Fitchburg, USA). Typically, 0.5 to 5 μg of kinase was pre-incubated with 10 μg of substrate (and inhibitor compounds, if using) in a total volume 25 μL in 20 mM Tris (pH 7.5), 20 mM $MgCl_2$, 2 mM $MnCl_2$, 1 mM DTT at 30ºC for 30 minutes. 10 μM of ATP (final concentration) was added to start reaction and incubated at 30ºC for another 30 minutes. The reaction was stopped by the addition of ADP-Glo™ (to deplete ATP) and detection was performed as described by the manufacturer. If assay was performed with inhibitor, this was added at the pre-incubation step (to allow time for binding to the kinase and equilibration with the assay condition). The inhibitor was added to a final concentration of 2 μM, in DMSO, (final DMSO concentration in the assay of ~1%). Determination of IC_{50} for compounds against specific kinases requires the construction of a log [1] vs %ATP used curve, from

which the point at which 50% inhibition occurs is extrapolated. Serial dilutions of the inhibitor were made, covering concentration range from 100 μM down to ~10 nM. This allows determination of IC_{50} within the low μM to mid-μM range, and a different range of inhibitor concentrations can be explored if the curve is shifted too far to one end of the dilution series.

9. Phenotypic analysis of compound-treated parasites by Giemsa-stained slide

Synchronized parasites (3D7, 2% parasitaemia in 3% hct) were prepared in 96-well plates when they were around 12 hpi. The parasites were then treated with EC_{95} of IPK_0002, 4, and 6, which were 1.25 μM, 2.5 μM, and 625 nM, respectively (5μL of compounds + 95 μL parasite culture). After each 12, 18, 24, and 36 h-drug exposure time, two wells were chosen randomly our of 10 replicates for smearing on slides, which were followed by fixing and staining using methanol and Giemsa solution (Merck, Whitehouse Station, USA), respectively. After dry out the slides, they were subjected under the microscope (eclipse E200, Nikon, Tokyo, Japan) to investigate parasitaemia and morphology. To know the compound effect on late stages, synchronized parasites (1% parasitaemia in 3% hct, 35 hpi) were prepared with the compounds in 96-well plates using the same way. After 18-h incubation, parasites from two wells were chosen randomly and preceded with the same procedures for preparing Giemsa-stained slides.

10. Image-based *Toxoplasma gondii* proliferation and invasion assay

U2OS cells (2000 cells in 50 μL per well) in a complete medium (CM) were added to 384-well plate (Greiner Bio-One) and incubated for 24 h to have confluency of 80-100%. Serially-diluted compounds (6 μL) ranging from 40 μM to 1.2 nM (two-fold dilution) were added onto the host cell, which was followed by an addition of parasites (12,000 parasites in 4 μL CM) in each well. The plates then were incubated for 32 h at 37^{o}C. After the drug exposure time, the cells and parasites were fixed and stained by adding 30 μL of a solution containing Draq 5 (Biostatus, Shepshed, UK) with 1:1000 dilution and 12% paraformaldehyde. After 3 h incubation at room temparature, the plates were washed using DPBS (Gibco) three times to remove residual staining solution and were preceded with image acquisition in Operetta (PerkinElmer). For invasion assay, the protocol was slightly modified. U2OS cells (10,000 cells in 50 μL) were seeded in a 96-well plate for 24 h at 37^{o}C. Serially-diluted compounds (5 μL) ranging from 100 μM to 45 nM (three-fold dilution) were added in each well, which was followed by a sequential addition of parasites (48000 parasites in 45 μL; 6 parasites per cell). After 2 h incubation at 37^{o}C, the plates were preceded with vigorous washing using mixing (Mixmate, 1,000 rpm, 30 sec) and aspiration, three times to remove residual compounds and extracellular parasites. After the washing, each well was filled with CM (100 μL) to be incubated for more 32 h at 37^{o}C. The parasites and cells were fixed and stained by staining solution (50 μL, 12% paraformaldehyde + 1:1000

diluted Draq 5), which was followed by image acquisition directly without washing out staining solution.

11. Molecular docking analysis

For docking calculations, the PbCDPK1 target protein (PDB code 3Q5I) was prepared using the protein preparation wizard in Maestro 8.0 (Schrödinger, NY, USA). Water from the active-site region was removed, as was the ADP ligand. Hydrogen atoms were added to the protein and hydrogen bonds were optimized to default values. Energy minimization in MacroModel 9.5 (Schrödinger) was performed only on the protein hydrogens using default parameters. A receptor grid, which is large enough to encompass all crystallographically observed binding sites was then generated from the prepared target protein. Geometry-optimized ligands were docked using Glide standard-precision (SP) mode, and no other constraints were applied.

Results

I. Primary Screening and Hit Selection

Primary screening

Aiming to find a *P. falciparum*-specific kinase inhibitor, which can be a potential candidate for a novel antimalarial drug in the future, I screened 4,000 compound collections, which were uniquely designed to target various kinases, onto *P. falciparum* 3D7 as well as Dd2, the multidrug-resistance strain. The assay used was SYBR Green I assay, estimating parasite viability via measuring DNA amount of parasites, was adapted in 384-well plates to improve screening throughput. The total of 32 plates covering 4000 compounds for respective 3D7 and Dd2 strains were set up in one day. Each plate contained 0.5% DMSO- and 400 nM artemisinin-treated wells for positive and negative controls, respectively, which were used for data normalization afterwards. As a result of primary screening, Fig. 2 shows the viability of Dd2 (x-axis) and 3D7 (y-axis) strain after the treatment of compounds at 10 μM for 72 h. The z-factors for the screening of 3D7 and Dd2 were 0.7 and 0.6, respectively, which inform a good enough separation between positive and negative controls, eventually enabling a reliable hit selection based on the controls. As expected, overall activities of the compounds were not the same for the two different strains; the activity was extremely different in some cases, where the compound was active over 90% on Dd2 while it showed less than 20% activity on

3D7 (Fig. 2, red arrow) or vice versa (Fig. 2, blue arrow). Since we are seeking for a kinase inhibitor that is potent for both wild type (3D7) and the drug resistant strain (Dd2), the compounds that had activities over 90% for both strains were selected and resulted in the selection of total 196 compounds (Fig. 2, blue square).

Filtering out cytotoxic compounds

The selected primary hits (total 196 compounds) were checked for their cytotoxicity in four human cell lines: U2OS, HeLa, THP1 and Huh7.5. The viability of the cells was checked at 10 μM of each compound as described in detail in "Materials and Methods" section. We considered as a cytotoxic compound when the viability in all four-cell lines showed less than 70%, which stringently removed 87 compounds from the primary hits and resulted in total 109 compounds, which was proceeded for further study.

Selection of highly active compounds based on their EC_{50}

The hits (109 compounds) that are active on *Plasmodium* but not toxic in human cells were confirmed for their efficacy on parasites using SYBR Green I assay via assessing an EC_{50} of each compound. The compounds were serially diluted ranging from 20 μM to 4.9 nM in 384-well plates and incubated with parasites (3D7 and Dd2) as detailed in "Materials and Methods" section. After the assay, dose-response curve of each compound was achieved and EC_{50} was calculated from the curve. Out of 109 compounds, 23 compounds were found to be highly active ($EC_{50} < 1$ μM) for

both 3D7 and Dd2 strain and to compose 5 different clusters after clustering analysis based on their common scaffolds (Fig. 3).

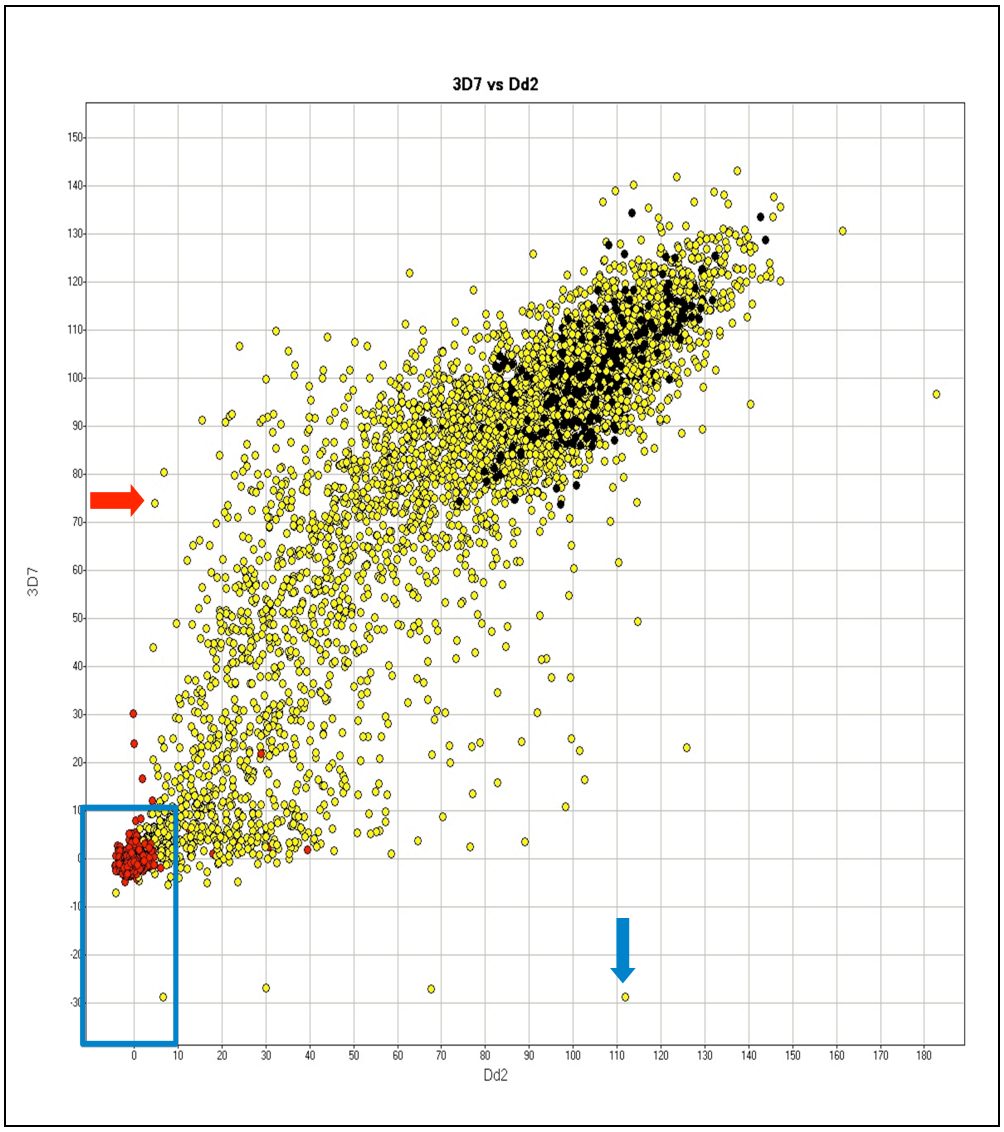

Fig. 2. Primary screening results comparing each compound's efficacy at 10 μM on *P. falciparum* 3D7 and Dd2.

Parasite cultures (3D7 and Dd2) were treated with each compound of the kinase-directed inhibitor library in 384-well plates at 10 μM for 72 h. After drug incubation

time, the plates were developed using SYBR Green I assay. The raw data were normalized based on 400 nM artemisinin (red dots) and 0.5% DMSO-treated wells (black dots) as negative and positive controls, respectively. The normalized viability of 3D7 and Dd2 for each compound (yellow dots) were plotted together to compare the compound's efficacy in a wild type (3D7) and a drug-resistant parasites (Dd2) using Spotfire. Compounds, as an example, where their efficacies were extremely different in the two strains are indicated with arrows (red and blue arrow). The selected compounds that are active over 90% for both 3D7 and Dd2 are shown in a blue square.

(A)

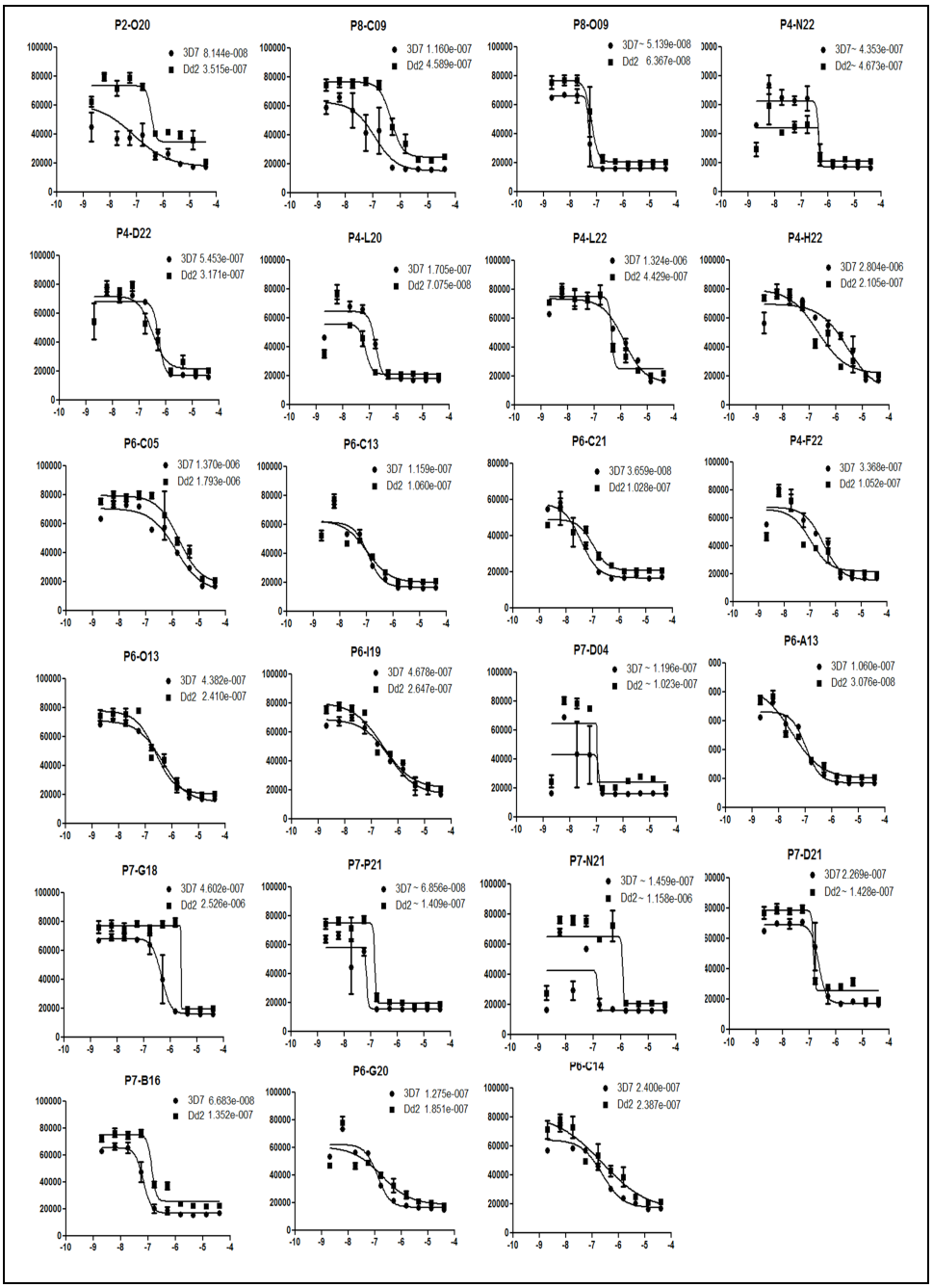

Figure 3. The compounds that are highly active (EC_{50} < 1 μM) for both *P. falciparum* 3D7 and Dd2.

(B)

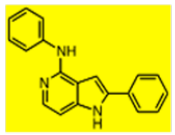

1

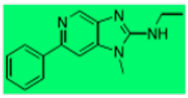

2

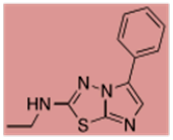

3

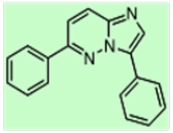

4

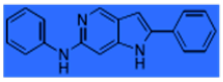

5

Compound ID	3D7 EC_{50} (μM)	Dd2 EC_{50} (μM)	3D7 SI	Dd2 SI
cnd_0091	0.23	0.14	> 43.5	> 142.9
cnd_0091*	0.07	0.14	> 143	> 142.9
cnd_0043*	0.35	0.7	> 28.6	> 14.3
cnd_0716*	0.12	0.1	> 83	> 100
cnd_0716	0.46	2.5	> 21.7	> 4.0
cnd_0087	0.05	0.6	> 200	> 167
cnd_0079	0.07	0.14	> 143	> 71.4
cnd_0135	0.12	0.46	> 83.3	> 21.7
cnd_4027	1.3	0.44	> 7.7	> 22.7
cnd_4027	0.5	0.3	> 20	> 33.3
cnd_4027	0.17	0.07	> 59	> 143
cnd_0168	0.34	0.1	> 29.4	> 100
cnd_0168	0.44	0.47	> 23	> 21
cnd_0168	2.8	0.2	> 3.6	> 50
cnd_0347*	0.24	0.24	> 42.7	> 42.7
cnd_0347	1.4	1.8	> 7.1	> 5.6
cnd_0081*	0.12	0.1	> 83.3	> 100
cnd_4145	0.44	0.24	> 22.7	> 41.7
cnd_6488	0.1	0.03	> 100	> 333
cnd_6488*	0.04	0.1	> 250	> 100
cnd_6488*	0.13	0.19	> 77	> 53
cnd_0312*	0.47	0.26	> 21.3	> 38.5
cnd_4308*	0.08	0.35	> 125	> 29

Figure 3. The compounds that are highly active (EC_{50} < 1 μM) for both *P. falciparum* 3D7 and Dd2.

(A) Dose-response curves of the highly active compounds. Serially diluted compounds ranging from 20 μM to 2.9 nM was prepared in 384-well plates (4-fold dilution) and incubated with parasite cultures (3D7 and Dd2) for 72 h. After the exposure time, the plates were preceded with SYBR Green I assay. The raw data were plotted in Prism 5.0 (Graphpad) to achieve dose-response curves for 3D7 and Dd2, respectively. The estimated EC_{50} for the two different strains are presented on the right-up side of each graph. (B) Clusters and their chemical scaffolds comprising the compounds that are highly active for 3D7 and Dd2. After clustering analysis, 5 clusters were found to be major scaffolds constituting the highly active compounds (EC_{50} < 1 μM). The each chemical scaffold is shown in the left side of the table in different colors. Selectivity index (SI) of the compounds for respective 3D7 and Dd2 are also shown and calculated based on the EC_{50}s and cytotoxicity data. The compounds chosen for a follow-up study are indicated by a remark (*).

II. Identification of a Kinase Target

Screening compounds on a panel of recombinant *Plasmodium* kinases using fluorescence-based thermal shift assay

Out of the highly active compounds (n=23), 9 compounds were selected (relabeled by Institute- Pasteur-Korea code) due to their availability and purchased for a follow-up study (Fig. 4A). Their activities were re-confirmed by SYBR Green I assay against the parasites and the dose response curves are shown in Fig. 4B. These IPK-labeled compounds (IPK compounds) were from cluster 1, 4, and 5, which were designed to be either ATP competitive (cluster 1) or non-ATP competitive (cluster 4) inhibitors, respectively. In an attempt to find a possible kinase target for IPK compounds, collaboration has been made with Dr. Christian Doerig from Monash University in Austrailia to have the compounds tested on their recombinant *Plasmodium* kinases (Table 1). Total 10 different *Plasmodium* kinases including 7 essential and 3 non-essential kinases for intra-erythrocytic phase, respectively, were screened against 9 IPK compounds at 5 μM using fluorescence-based thermal shift assay (FTA) (Fig. 5). This assay enables to select compounds that are able to bind to the enzyme stably, eventually improving the stability of the protein compared to the native protein. As a result, 8 IPK compounds were found to have affinity for PfCDPK1 (*P. falciparum* calcium-dependent protein kinase 1), PfNek2 (*P. falciparum* NIMA-related kinase), PfPK7 (*P. falciparum* protein kinase 7), and PfCK2 (*P. falciparum* casein kinase 2). While some enzyme such as PfNek2

had promiscuous hits, PfCDPK1 had three compounds (IPK_0002, 4, and 6) that showed potent binding (Fig. 5A). It's not surprising that the three compounds belong to the same cluster (cluster 4). Interestingly, these compounds had the same binding specificity onto PfPK7, however, it is unlikely to be a real target because it is not an essential enzyme for *P. falciparum*. Therefore, I decided to focus on the IPK_0002, 4, and 6, which showed the most potent affinity to the PfCDPK1 and continued to prove that the target is PfCDPK1.

Effects of the compounds on recombinant PfCDPK1 activity

In order to investigate if the three compounds (IPK_0002,4, and 6) are truly targeting a kinase, PfCDPK1, not simply binding to it, the compounds were further tested if they could inhibit kinase activity of the recombinant PfCDPK1. PfCDPK1 and the compounds were incubated with ATP as well as its substrates. The kinase activity was estimated by measuring ADP amount released after the kinase reaction. Indeed, the compounds showed inhibition effects on the recombinant PfCDPK1 in a dose-dependent manner (Fig. 6). The estimated IC_{50} was 0.5, 5 and 1.8 μM for IPK_0002, 4, and 6, respectively, which were higher compared with their cellular activities (EC_{50}).

Effects of the compounds during *P. falciparum* life cycle

After knowing the enzyme target of the compounds, I wondered how they alter parasite's phenotype by targeting PfCDPK1 even though I already knew that these compounds were the hits from viability screening. First, to know the phenotypic

effect during parasite's developmental stage, I synchronized parasites (3D7) using two-sequential sorbitol treatment (8 h interval) and released the ring-stage parasites into medium containing the compounds at their EC_{95} (1.25 μM, 2.5 μM, and 625 nM, respectively for IPK_0002, 4, and 6) concentrations. Then, some samples of treated and untreated parasites were stained with Giemsa, respectively in different time points to check their parasitaemia and morphology. As shown in Fig. 7, the untreated parasites progressed from ring to trophozoite and schizont stages through the cell cycle whereas the compound-treated parasites arrested at ring stage after 12-h incubation. The compounds kept parasites arrested in early stages during the life cycle while untreated parasites were able to reinvade red blood cells, resulting in increased parasitaemia in 36-h incubation.

It is known that the gene of PfCDPK1 appears to be expressed from the onset of schizogony (30-35 hpi) and the protein accumulates in the cell until the end of the cycle. [31]. Thus, I next wanted to check the direct effect of the compounds on the late-schizont parasites. Parasites (3D7) were synchronized using the same method but this time the compounds were applied to only late-stage parasites (~35 hpi) and incubated for 18 h until the parasites form rings (~13 hpi) after the following invasion. As a result, the compound-treated parasites were not able to progress their life cycle and failed to egress and re-invade new red blood cells while untreated parasites were successfully developed and underwent invasion process (Fig. 8).

Effect of the compounds on a-related parasite, *Toxoplasma gondii*

Calcium-dependent protein kinases (CDPKs) are only found in some plants and apicomplexan protozoa that includes malaria parasites *Plasmodium spp*. as well as *T. gondii*, which is responsible for toxoplasmosis. Recent data showing the CDPK1 is involved in parasite motility and host cell invasion [31,32,33], which is essential process for the parasite, have made this enzyme as an attractive drug target. I first wanted to know if the compounds targeting PfCDPK1 could also work in a-related-parasite, *T. gondii.* Prior to test this possibility, a cell-based assay was developed to visualize the drug effect on the growth of *T. gondii.* As demonstrated in Fig. 9, extracellular tachyzoite parasites (6 parasites per cell) were added on the top of U2OS cells and allowed to invade and proliferate inside the host cells for 36 h. In *in-vitro* culture system, *T. gondii* multiplies by two every 8 h, thus, theoretically being a total 96 parasites inside a cell by the end of the incubation time. After the drug incubation time, the cells and parasites were stained using DNA dye (Draq5). Phenotypic effect from each well by the compounds was assessed by imaging using automatic-fluorescence microscope and the images were analyzed by specific software developed in house. The software can count the number of parasite-infected cells over total number of cells to calculate "infection ratio". As a result, Fig. 10 shows that the three compounds appeared to be active on *T. gondii* with estimated EC_{50} of 2.9 μM, 5.2 μM, and 5 μM, respectively for IPK_0002, 4 and 6. However, besides the activities on the parasites, they showed toxicities on the host cells (Fig. 10, blue curve from each graph).

After knowing the compounds worked in *T. gondii,* I wondered if the compounds could inhibit parasite's invasion process since CDPK1 has been implicated in

parasite motility and invasion in recent studies [32,33]. Thus, I promptly modified the assay in order to observe the effect of the compounds specifically on the invasion process (Fig. 11A); after parasites and the compounds were added on the host-cell plate, they were allowed to invade cells for 2 h, then the medium containing free parasites and compounds was subsequently washed out from the plate so that only invaded parasites can progress the life cycle inside the cell. The successfully invaded parasites will grow for the same hours (36 h). As a result, the compounds indeed inhibited parasite's invasion specifically and showed EC_{50} with 2.2 μM, 4.3 μM, and 4 μM, respectively for IPK_0002, 4, and 6, which were the very similar potencies that we observed in the *T. gondii*-growth inhibition assay (Fig. 11B-D). Furthermore, in the invasion assay, it was clear to see the inhibition effects on the invasion process because no adverse cytotoxic effect was observed due to the short drug exposure time (2 h).

A

1

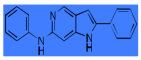

4

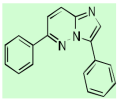

Novel-binding mode

5

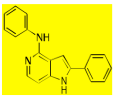

Hinge-binding mode

Compound ID	3D7 EC_{50} (μM)	Dd2 EC_{50} (μM)	3D7 SI	Dd2 SI
IPK_0001	0.54	2.5	>18.5	> 4
IPK_0002	0.02	0.1	> 500	> 100
IPK_0003	0.16	0.3	> 62.5	> 33
IPK_0004	0.4	0.5	> 18.5	> 20
IPK_0005	0.54	1.1	> 18.5	> 9.1
IPK_0006	0.06	0.08	> 167	> 125
IPK_0007	0.32	0.9	> 31.3	> 11.1
IPK_0008	0.1	0.2	> 100	> 50
IPK_0009	0.15	0.28	> 67	> 36

B

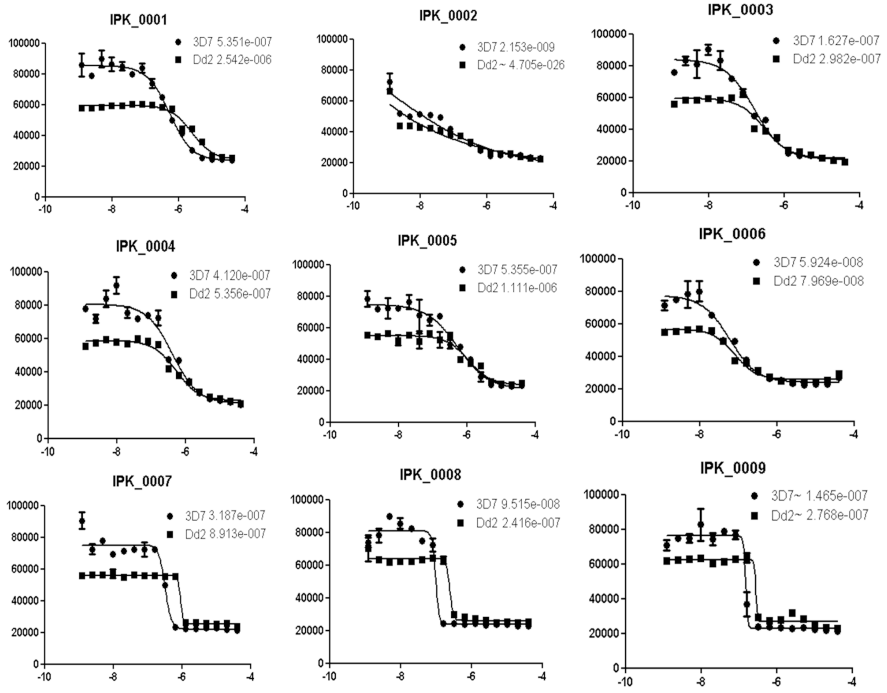

Fig. 4. Purchased and relabeled compounds for a further study.

(A) List of the compounds that finally were selected and purchased for a follow-up study. Out of 23 compounds that were highly active ($EC_{50} \leq 1$ μM) for *P. falciparum* 3D7 and Dd2, 9 compounds constituting cluster 1, 4 and 5 were further chosen and re-labeled by IPK code (from 0001 to 0009). (B) Prior to the further study, they were re-confirmed by assessing EC_{50}s using SYBR Green I assay. Serially diluted compounds ranging from 40 μM to 1.2 nM (two-fold dilution) were treated onto the parasites (3D7 and Dd2) and preceded under the same protocol as the "Hit confirmation" step detailed in "Materials and Methods" section.

(A)

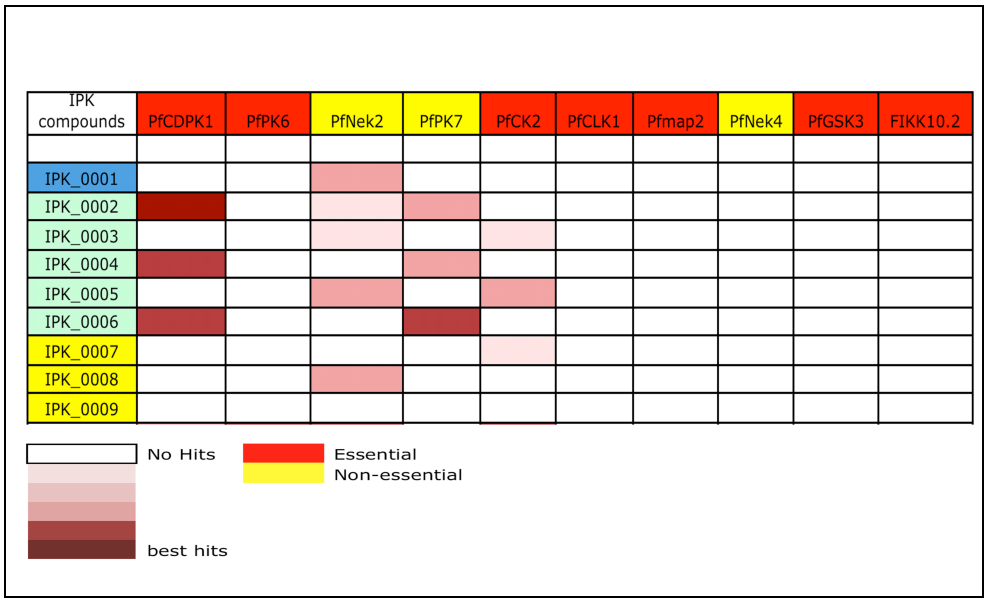

(B)

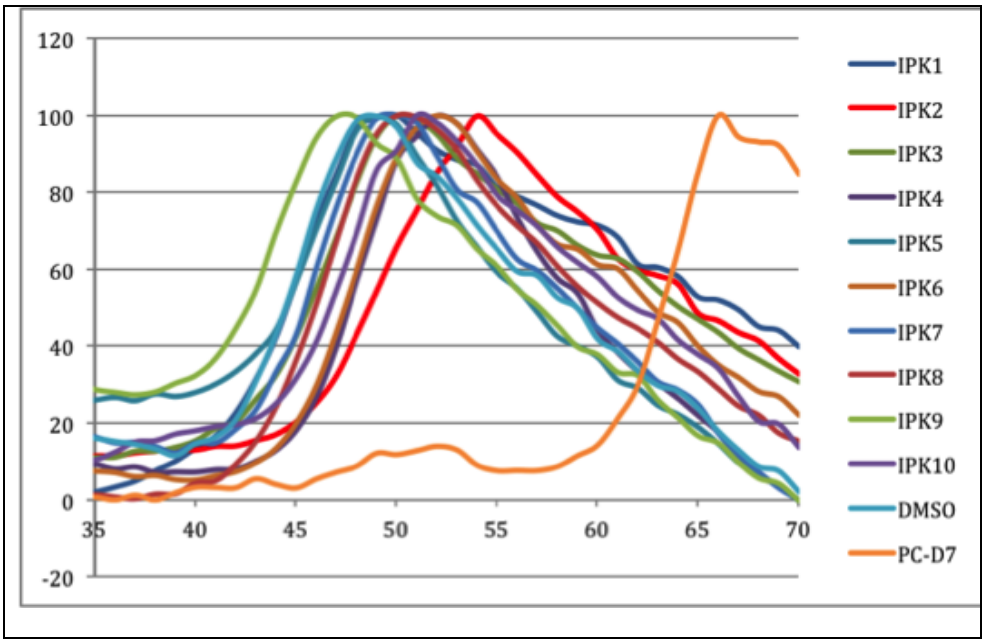

Fig. 5. Screening IPK compounds against recombinant *Plasmodium* kinases.

IPK compounds were screened against recombinant and purified *Plasmodium* kinases at 5 μM using Fluorescence-based thermal shift assay (FTA). (A) The kinases tested include 7 essential and 3 non-essential enzymes for intra-erythrocytic phase of *Plasmodium* life cycle (indicated in red and yellow color, respectively). The hits are represented in russet with scale. (B) The curve of FTA for each compound onto the PfCDPK1. Each curve indicates each compound in different colors as well as positive and negative controls.

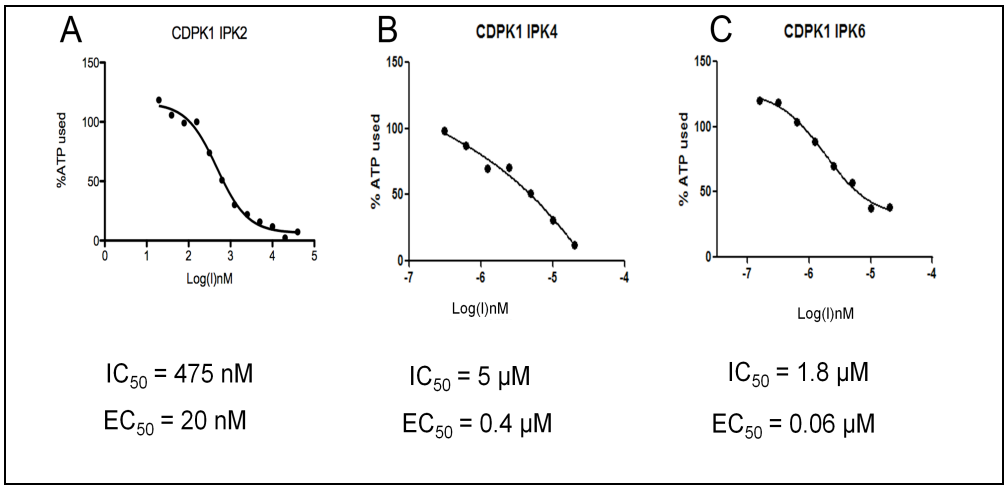

Fig. 6. Effects of the compounds on recombinant PfCDPK1 activity.

IPK_0002 (A), IPK_0004 (B), and IPK_0006 (C) were tested onto recombinant PfCDPK1 using kinase assay (ADP-Glo™) as described in "Materials and Methods" section. Kinase reaction was performed with each compound ranged from 100 μM to 10 nM (two-fold dilution), which was followed by a detection of a released ADP amount, which was converted into % ATP used finally. The dose-response curve of each compound was prepared using Prism 5.0 (Graphpad). EC_{50} data of compounds from viability assay are also shown to compare with their IC_{50}.

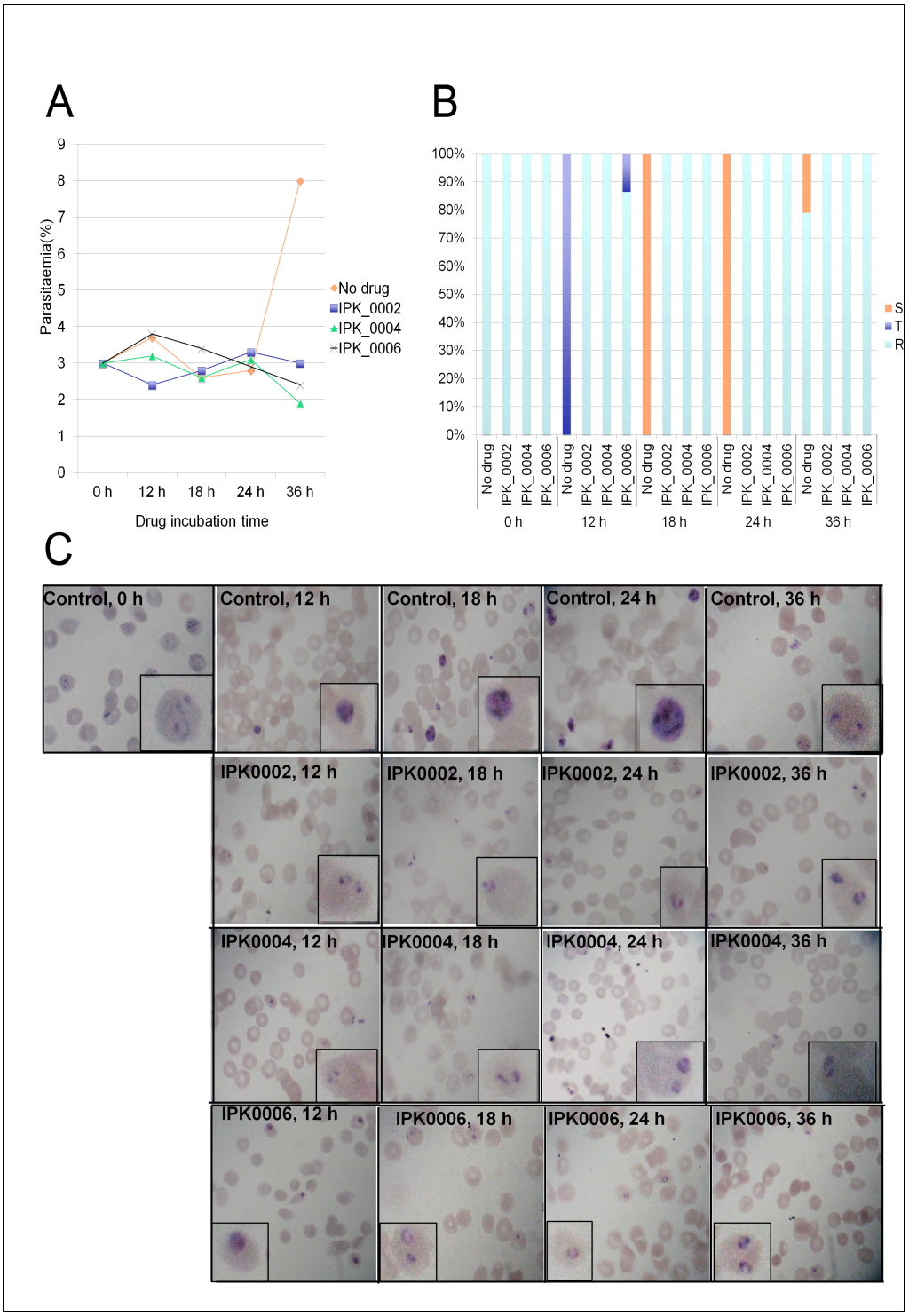

Fig. 7. Effects of the compounds on *P. falciparum* life cycle.

P. falciparum 3D7 was synchronized with a double synchronization method with sorbitol treatment and ring-stage parasites (12 hpi) were set up in a 384-well plate as control. Compounds (IPK_0002,4,and 6) were treated onto the same parasites by adding EC_{95} of each compound per well (volume ratio of compound: parasite = 5 μL : 95 μL). The untreated and treated parasites were checked for their parasitaemia (A) and stage proportions (B) in different time points (S: Schizonts, T: Trophozoites, R: Rings). In each time point, parasite cultures from 3 different wells were mixed up to prepare slides. The parasites onto the slides were fixed with methanol and stained using Giemsa-staining solution, which was followed by analysis under the microscope (C).

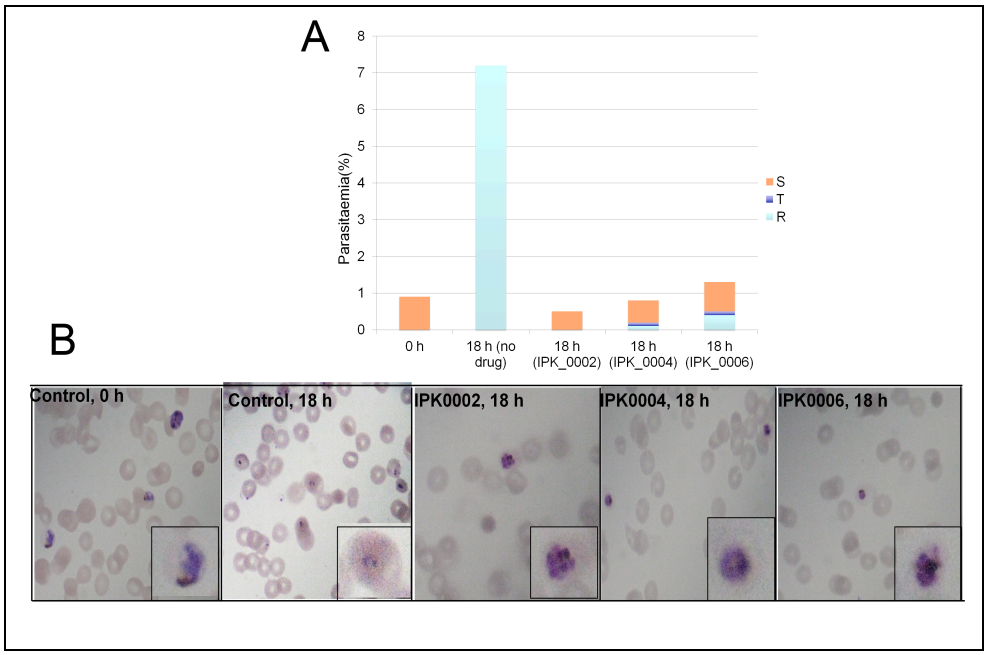

Fig. 8. Effects of the compounds on *P. falciparum* late schizogony.

P. falciparum 3D7 was synchronized with a double synchronization method with sorbitol treatment and schizont-stage parasites (~35 hpi) were set up in a 384-well plate as control. Compounds (IPK_0002,4,and 6) were treated onto the same parasites by adding EC_{95} of each compound per well (volume ratio of compound: parasite = 5 μL : 95 μL). The untreated and treated parasites were checked for their parasitaemia (A) and morphology (B) after 18-h incubation. Parasite cultures from 3 different wells were mixed up and smeared on slides. The parasites on the slides were fixed with methanol and stained using Giemsa-staining solution prior to observation under the microscope .

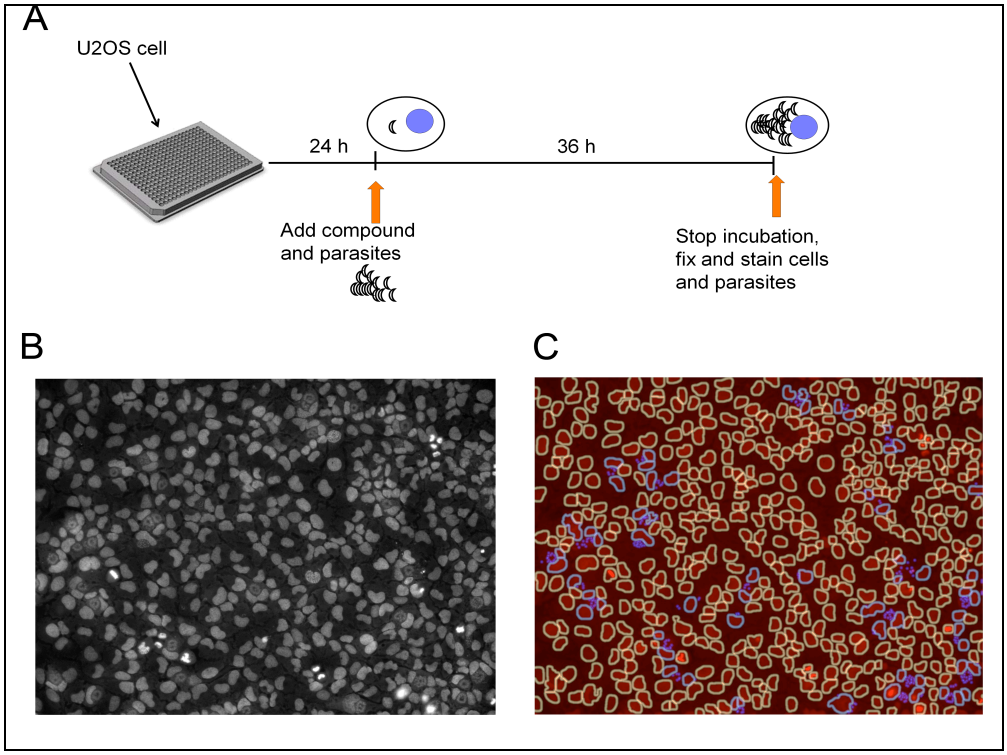

Fig. 9. Scheme of an image-based *T. gondii* proliferation assay.

(A) Overall scheme of the assay shows U2OS cells (2000 cells per well) were added in 384-well plate and incubated for 24 h at 37°C, which was followed by adding compounds and parasites (6 parasites per cell) subsequently. The plates were incubated for more 36 h until the parasite invaded host cells and multiplied inside them. Before the host cell rupturing by parasites, incubation was stopped and the parasites as well as cells were fixed and stained by 4% paraformaldehyde and Draq5, respectively. The plates underwent image acquisition process (Operetta) and the raw images (B) were analyzed by in-house software (C) that detects uninfected cells and infected cells as yellow and purple color, respectively.

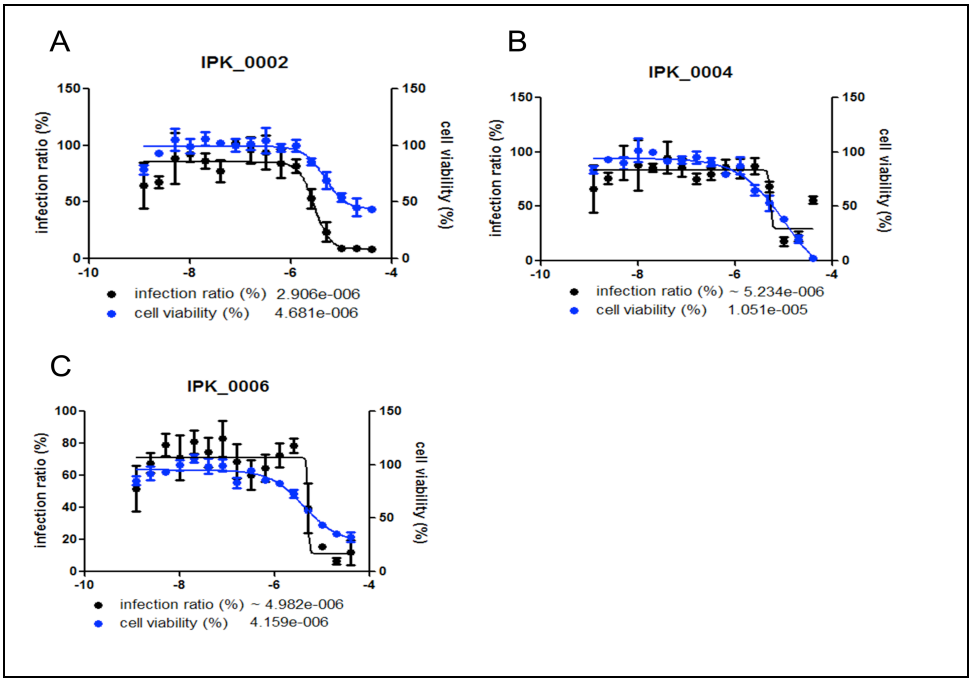

Fig. 10. Effects of the compounds on the growth of *T. gondii.*

Serially diluted compounds IPK_0002 (A), IPK_0004 (B), and IPK_0006 (C) ranging from 40 μM to 1.2 nM were tested on *T. gondii* using an image-based parasite proliferation assay as described in detail in "Materials and Methods" section. After the assay, the images from each plate were acquired by automatic microscope system (Operetta) and analyzed by specific software that was developed in house. The software calculated the number of infected cells over total number of cells to express "infection ratio (left-y axis)" and "cell viability (right-y axis)" that showed in each graph. The raw data were normalized based on positive (DMSO-treated wells) and negative (Pyrimethamin-treated wells) controls prior to presenting the curves (Prism 5.0). Estimated EC_{50} and CC_{50} are shown in right below the graphs.

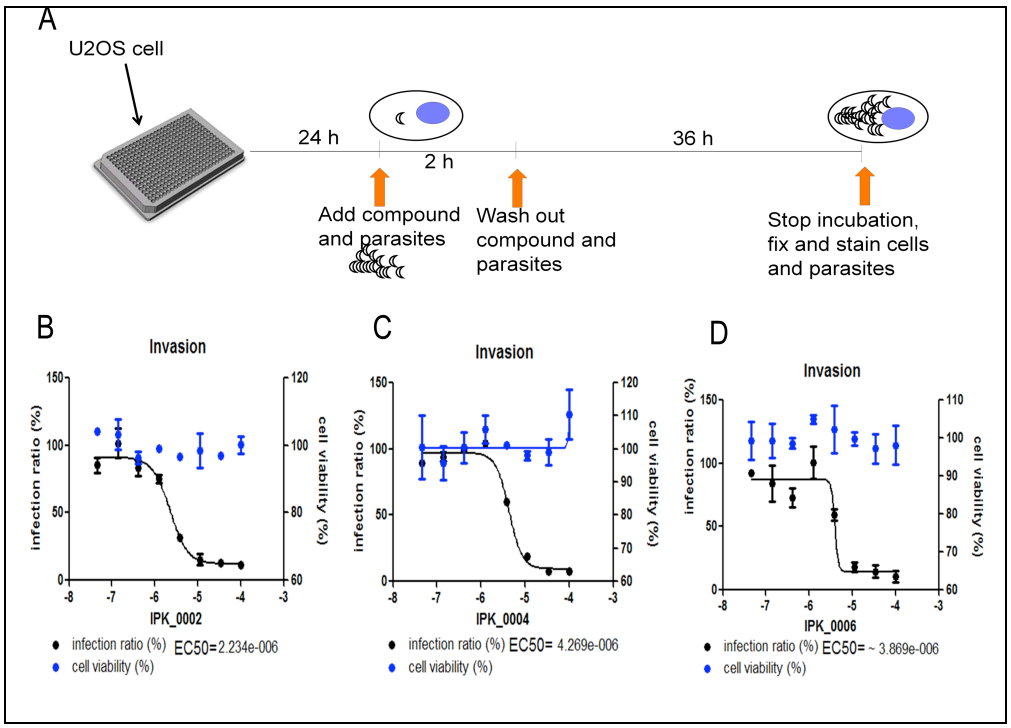

Fig. 11. Effects of the compounds on *T. gondii* invasion.

(A) Scheme of *T. gondii* invasion assay, which was slightly modified from the image-based *T. gondii* proliferation assay. The parasites and serially diluted compounds ranging from 100 μM to 45 nM (three-fold dilution) were added onto U2OS cells in 96-well plate. The plates were incubated for 2 h for allowing invasion of the parasites, which was followed by intensive washing out (Mixmate) of un-invaded parasites and residual compounds. The successfully invaded parasites continued to grow for 36 h before fixing and staining them. (B-D) Results of the invasion assay using the compounds. The images from well plates (Operetta) were analyzed by specific software and the infection ratio was calculated based on the number of infected cells over total number of cells. The data were normalized

afterwards based on DMSO-treated wells and Pyrimethamine-treated wells as positive and negative controls, respectively. The dose- response curves were prepared using Prism 5.0 and the estimated EC_{50}s are shown in below the graghs.

Table 1. *P. falciparum* kinases expressed and purified in this study. Their essential characteristics are indicated for *P. berghei* and *P. falciparum*, respectively

PlasmoDB	Name	Group	Phenotype		Tested domain
			P. berghei	*P. falciparum*	
PFB0815w	PfCDPK1	CDPK	Essential	Essential	Full-length
MAL13P1.185	PfPK6	CMGC/CDK	Essential	Essential	Full-length
PF11_0096	PfCK2	CMGC(CK2)	Essential	Essential	Full-length
PF0525c	PfGSK3	CMGC(GSK3)	Essential	Essential	Full-length
PF14_0431	PfCLK1(Lammer)	CMGC/CDK-like	Essential	Essential	Kinase domain
PF10_0380	FIKK10.2	FIKK-orphan	ND	Essential	Kinase domain
PF11_0147	Pfmap2	CMGC,MAPK	Male gamete defect	Essential for erythrocytic stage	Full-length/kinase domain
PFB0605w	PfPK7	Orphan	Oocyst Maturation	Not Essential for erythrocytic stage	Full-length
PFE1290w	PfNek2	CMGC,Nek	Ookinete defect	Not Essential for erythrocytic stage	Full-length
MAL7P1.100	PfNek4	CMGC,Nek	Oocyst Maturation	Not Essential for erythrocytic stage	Full-length

III. Molecular Docking Analysis

To understand the binding mode of the compounds to CDPK1, *in silico* molecular docking analysis was performed using the known CDPK1 structure. Currently, the structures of CDPK1 from different sources are available in Protein Data Bank (PDB, www.rcsb.org); CDPK1 structures from *T. gondii, Cryptosporidium parvum,* and *Plasmodium bergei* are already disclosed. CDPK1 from *P. bergei* (PDB code 3Q5I) was chosen for the analysis due to the high sequence homology (sequence homology between PfCDPK1 and PbCDPK1 is ~88%). The compounds targeting PfCDPK1 are shown in Fig. 12. The compounds share the core scaffold, which is a derivative of imidazopyridazine. Prior to docking the compounds onto PbCDPK1, the binding mode of ATP in the active site of PbCDPK1 was first checked using MacPyMOL. The ATP was observed to provide with two hydrogen bonds to the hinge region of the PbCDPK1 (Fig. 13). The compounds were then docked into the active site of PbCDPK1 and interestingly showed a different feature from ATP, where none of the compounds showed interaction with the hinge region of the protein (Figure 14). Rather, in case of IPK_0004 and IPK_0006, they interacted with T144 and R61 of the protein in the backside of the hinge, respectively via hydrogen bonds. These features might be due to the calcium existing in the catalytic site of the protein, attracting the atom like oxygen or sulfur that has unshared electron pair from the compounds, thereby, positioning the imidazopyridazine

moiety, which could have interacted with the hinge otherwise, apart from the hinge region (Fig. 14).

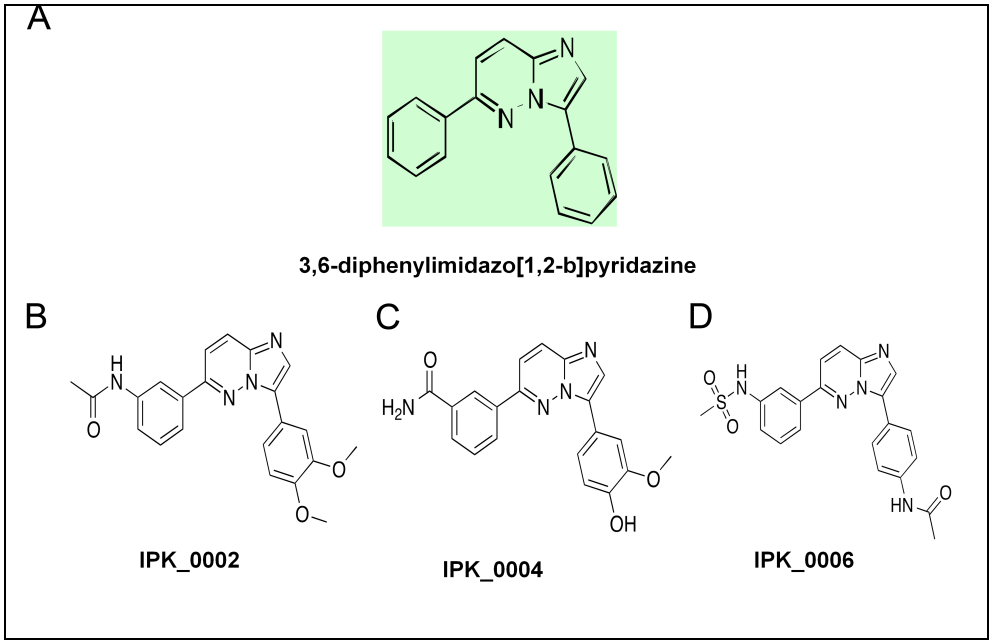

Fig. 12. The structures of the three compounds and their core scaffold.

The structure of the shared scaffold of the three compounds are shown (A), which is derivative of imidazopyridazine. (B-D) The structure of the three compounds used in this study.

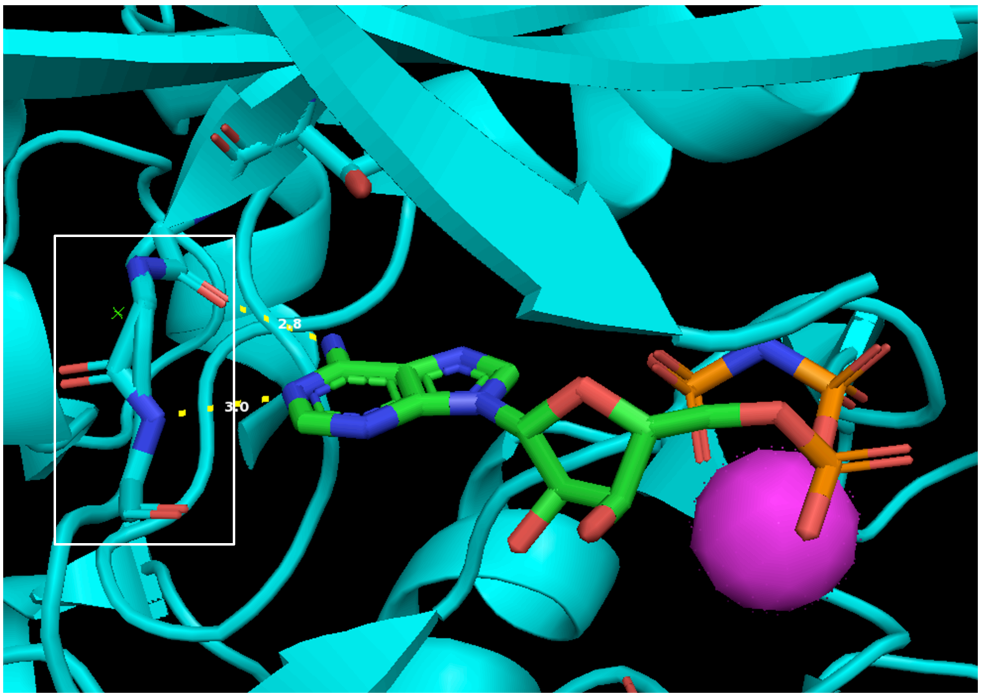

Fig. 13. The ATP binding mode in PbCDPK1 (PDB code 3Q5I).

ATP-binding mode in the catalytic site of the PbCDPK1 (PDB code 3Q5I) are shown using MacPyMOL. Hinge region is indicated in white box, which providing with two hydrogen bonds to ATP. Purple sphere represents calcium, blue and red atoms represent nitrogen and oxygen, respectively.

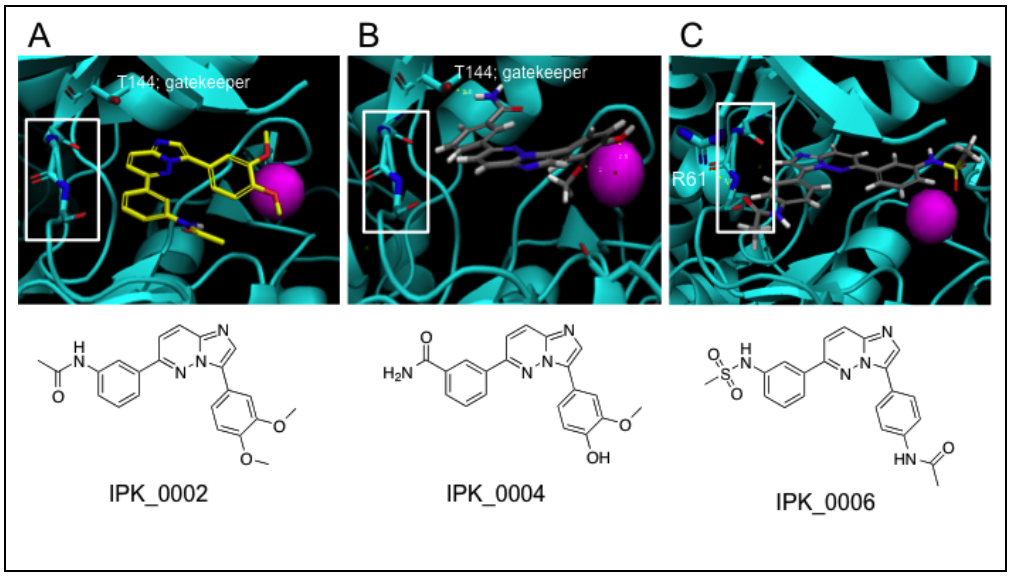

Fig. 14. Structure-based molecular docking analysis.

In silico molecular docking analysis between our compounds and PbCDPK1 revealed a mode of binding different from ATP, where typically provides two or three hydrogen bonds to hinge region of active sites. The protein structure was loaded from PDB (PDB code 3Q5I) and the docking was performed as explained in "Materials and Methods" section. Hinge region is indicated in white box, purple sphere represents calcium. The atoms of nitrogen and oxygen show in blue and red color, respectively. The typical gate keeper residue of the kinase is indicated and MacPyMOL was used to generate A-C.

Discussion

I have screened 4,000 kinase-directed chemical compounds, which were uniquely designed to target various kinases, using a cell-based phenotypic assay, SYBR green I assay. For a classical drug discovery perspective, which is target-based approach, the strategy here might be a challenge, where I started chemical-library screening directly in the parasites without knowing the target. However, evidences that show (i) the higher number of first-in-class drugs were discovered using phenotypic screening compared to target-based screening [36] and (ii) a subsequent failure of small molecules to be efficacious in intracellular context despite its high selectivity for its enzyme target [37,38], have rendered phenotypic screening acceptable as a more logical approach. Moreover, the target identification, which is the tricky part of phenotype-based drug discovery, was facilitated in this study by a screening the hit compounds against several recombinant *Plasmodium* kinases that were kindly provided by Dr. Christian Doerig.

I have successfully identified 23 small molecules that are potent (EC_{50}< 1 μM) for both the drug susceptible strain, *P. falciparum* 3D7 and the drug resistant strain, Dd2 whereas they have low toxicity in human cells (Fig. 3). These results might accelerate the drug discovery process by positioning the hits in candidates to be a good lead. Furthermore, in an effort to find a possible target, some of the hits were found to be able to bind to *Plasmodium* recombinant kinases to improve the enzyme

stabilities; 4 kinases (PfCDPK1, PfPK7, PfNek2 and PfCK2) were identified for 8 compounds (Fig. 5). Of these, I focused on the PfCDPK1 that showed the most potency for the three compounds (IPK_0002, 4, 6). The three compounds were also found as hits for PfPK7 in the fluorescence-based thermal shift assay (FSA), however, PfPK7 was unlikely to be a real target for the compounds because it is not an essential kinase for the parasite (remind that the compounds are the hits from viability screening). The compounds were next applied in the kinase assay to check their inhibition activity against recombinant PfCDPK1. In this assay, kinase activity was evaluated by measuring ADP amount released after the kinase reaction and the three compounds indeed inhibited efficiently recombinant PfCDPK1 activity in a-dose-dependent manner (Fig. 6). In addition, this implies that the three compounds competed with ATP in the kinase reaction; they are ATP-competitive-kinase inhibitors. The estimated IC_{50} of the compounds appeared to be relatively higher than their cellular activities (EC_{50}), however, this is not surprising because we normally add excessive amount of substrates and enzymes in the kinase reaction compared to their actual amount in a cellular context, which is very small [31]. Taken together, these data show that the compounds, IPK_0002, 4, and 6, which came out from the parasite viability screening are actually targeting parasite's essential kinase, PfCDPK1.

The gene of PfCDPK1 appears to be expressed from the onset of schizogony and peaks in late schizont stage. The protein accumulates in the cell until the end of cycle and the free merozoites after mature schizonts are ruptured [31]. In the present

study, the compounds blocked development of late schizonts when they were applied to ~35 hpi parasites, thereby, inhibiting parasite egress and the subsequent invasion event (Fig. 8). A similar phenotype was observed previously that a specific inhibitor against recombinant PfCDPK1 blocked schizont development (schizont segmentation to generate merozoites) [32]. These results suggest that the compounds have strong effect on the late schizont stage where the majority of PfCDPK1 is expressed, which is consistent time for the expression of its two substrates, PfGAP45 and PfMTIP that are the components of motor complex that plays critical role for merozoite invasion [31]. On the other hand, in this study, the compounds arrested parasites at the early stages when they were applied to ring-stage parasites (Fig. 7), therefore, there is a possibility that the compounds might also target another enzymes that are expressed in early stage (remind the compounds had affinity to recombinant PfPK7 as well, Fig. 5).

The molecular mechanisms powering motility appear to be similar in zoites of apicomlexa where they all have the conserved secretary organelles at their apical end such as micronemes, dense granules and rhoptries [40]. In this study, a-related-apicomplexan parasite, *T. gondii* was used to understand better the phenotypic effect of the PfCDPK1 inhibitors in the parasite invasion. Prior to test this possibility, the compounds were first confirmed for their activities in *T. gondii*-growth inhibition. To visualize the phenotypic effect, an image-based assay was developed along with a specific plug-in that differentiates parasite-infected cells from non-infected cells. The software provides two kinds of information (i.e.

infection ratio and cell viability) simultaneously after each image analysis. The compounds were confirmed their activities in *T. gondii*-growth inhibition, however, at the same time were cytotoxic for the cells (Fig. 10). This is interesting because the compounds appeared to be toxic for parasite-infected cells whereas they were safe enough when the cells were situated alone with the compounds (remind the compounds were selected from cytotoxic ones previously). This shows the phenotype of host cells can be altered by invaded parasites.

After knowing that the compounds worked in *T. gondii*, they promptly tested in *T. gondii*- invasion assay. When the compounds were tested on extracellular tachyzoites of *T. gondii,* they prevented parasites from invading host cells and the effects showed dose-dependent manner (Fig. 11). This supports that these three particular compounds are targeting the CDPK1, which is important for parasite motility and invasion that are highly conserved among apicomplexan parasites [32,41,42]. Consistent with this observation, previous studies also showed a tri-substituted purine, purfalcamine, which emerged from a screen as a potent inhibitor of recombinant PfCDPK1 *in vitro*, blocked *T. gondii* invasion [32].

After the cellular target of the compounds turned out to be PfCDPK1 from both the enzyme-based and cell-based assay, molecular docking analysis was performed to understand the binding mode between the compounds and the target protein. Of the known CDPK1 crystal structures, CDPK1 from *P. berghei* (PDB code 3Q5I) was used for the analysis due to its high similarity with PfCDPK1. The three compounds

share imidazopyridazine moiety as a core scaffold (Fig. 12). Prior to the docking of the compounds, ATP binding mode for PbCDPK1 was first confirmed (Fig. 13). As expected, the adenosine base of the ATP was interacted with hinge region of the enzyme via hydrogen bonds. This shows the typical kinase active site (ATP-binding site) that has been mimicked by the ATP-competitive kinase inhibitors developed to date; the hinge region provides normally with two or three hydrogen bonds to kinase inhibitors [35]. Interestingly, however, in molecular docking analysis using the three compounds, they appeared to have different binding mode from conventional kinase inhibitors and showed the interaction with calcium and backside residues rather than the kinase hinge region (Fig. 14). This feature might give a new insight to design kinase inhibitors targeting CDPK1, which could have ATP-competitive but not ATP-mimetic mode. Consistent with this observation, the core moiety of the compounds, imidazopyridazine has been recently found to provide a novel binding mode in the kinase active site of kinase PIM-1, where the compound binds to the catalytic lysine residue, making no obvious contact with the hinge region [34]. Taken together, however, additional enzyme-based biochemical data and the PfCDPK1 crystal structure with the compounds will have to be elucidated to confirm the actual binding modes of the compounds in the future.

Calcium-dependent protein kinase 1 (CDPK1) is very unique enzyme in apicomplexan parasites, being absent in animal cells and essential for the parasites with regulating parasite motility and invasion. Thus, it has been an attractive therapeutic target. After the crystal structure of the enzyme from *T. gondii* was

unveiled [43], the efforts to find a selective inhibitor of the enzyme have been made in several groups [44,45,46] with taking an advantage of unique glycine gatekeeper residue in the ATP-binding site of TgCDPK1. For *P. falciparum* CDPK1, with the lack of crystal structure as yet, a few efforts was done to find selective inhibitors: i) Kato *et al.* identified purfalcamine (a 2,6,9 tri-substituted purine) targeting PfCDPK1, which is very similar with known inhibitor, purvalonol B [32]. ii) Lemercier *et al*. developed potent *in vitro* inhibitors of CDPK1, which were not tested however in parasite cultures [47]. In the present study, three compounds are proposed as having a new structure as yet that are potent for *P. falciparum* 3D7 and Dd2 by targeting PfCDPK1. However, there was shown, in this study, the possibility that the three compounds might also target another enzyme not only target PfCDPK1. Therefore, to be a good lead, the compounds will have to be improved for their specificity on PfCDPK1 with the aid of medicinal chemistry in the future.

CDPK1 is an attractive target in view of the facts that it is highly conserved among apicomplexan parasites such as *Plasmodium, T. gondii*, and *C. parvum*. Thus, it might be possible to cure more than one disease using one drug by targeting CDPK1. To test this possibility, the compounds will have to be tested in the other two parasites. In the present study, however, the three compounds targeting PfCDPK1 were cytotoxic to *T. gondii*-infected cells (Fig. 10), although they showed the clear inhibition effect on the *T. gondii* invasion. Therefore, further efforts will be needed by medicinal chemistry to improve cytotoxicity of the compounds for *T.*

gondii, eventually to make an attractive universal drug that is able to treat several diseases at the same time in the future.

CDPKs exist as a family in a species; there are five CDPKs in *P. falciparum* (CDPK1-5) [42]. Individual CDPKs of *P. falciparum* are differently expressed in different stages of the parasite's life cycle and have distinct functions at these times. For example, PfCDPK4 is expressed in the asexual blood stage but it is not essential for the development of this stage parasites. However, it is essential for male gametogenesis [48]. Both CDPK2 and CDPK5 are detectable in asexual blood stages where CDPK5 has been proposed to have a role in the controlled secretion of the subtilisin-like protease SUB1 from the exonemes at the end of schizogony [49]. CDPK3 has been shown to be essential for gliding motility of ookinetes [50]. Therefore, it will be also good idea to test the three compounds targeting PfCDPK1 in this study in other CDPKs of *P. falciparum* to see their activities, thereby, aiming for a more potent molecule killing *P. falciparum* by targeting different stages of the parasite simultaneously in the future.

In conclusions, here the three compounds will definitely help for designing a new antimalarial drug targeting PfCDPK1 due to their new chemical structure. Furthermore, they are highly potent in *P. falciparum* 3D7 as well as the drug resistance strain, Dd2. The resistance for all the currently available antimalarial drugs has been reported today, therefore, a new candidate for an antimalarial drug is urgently needed. In this urgent situation, the three compounds here will provide an

important insight in the future for developing novel kinase inhibitors to facilitate the anti-malarial drug discovery, which desperately needs “something new”.

References

1. WHO (2010) World Malaria Report 2010.
2. Murray CJ, Rosenfeld LC, Lim SS, Andrews KG, Foreman KJ, et al. (2012) Global malaria mortality between 1980 and 2010: a systematic analysis. Lancet 379: 413-431.
3. Renia L, Wu Howland S, Claser C, Charlotte Gruner A, Suwanarusk R, et al. (2012) Cerebral malaria: Mysteries at the blood-brain barrier. Virulence 3(2): 193-201.
4. Umbers AJ, Aitken EH, Rogerson SJ (2011) Malaria in pregnancy: small babies, big problem. Trends Parasitol 27: 168-175.
5. Carter R, Miller LH (1979) Evidence for environmental modulation of gametocytogenesis in *Plasmodium falciparum* in continuous culture. Bull World Health Organ 57 Suppl 1: 37-52.
6. McKenzie FE, Bossert WH (1997) The dynamics of *Plasmodium falciparum* blood-stage infection. J Theor Biol 188: 127-140.
7. Mather MW, Darrouzet E, Valkova-Valchanova M, Cooley JW, McIntosh MT, et al. (2005) Uncovering the molecular mode of action of the antimalarial drug atovaquone using a bacterial system. J Biol Chem 280: 27458-27465.
8. Majori G (2004) [Combined antimalarial therapy using artemisinin]. Parassitologia 46: 85-87.
9. Parija SC, Praharaj I (2011) Drug resistance in malaria. Indian J Med Microbiol 29: 243-248.
10. Fidock DA, Nomura T, Talley AK, Cooper RA, Dzekunov SM, et al. (2000) Mutations in the *P. falciparum* digestive vacuole transmembrane protein PfCRT and evidence for their role in chloroquine resistance. Mol Cell 6: 861-871.
11. Hyde JE (2002) Mechanisms of resistance of *Plasmodium falciparum* to antimalarial drugs. Microbes Infect 4: 165-174.
12. Gregson A, Plowe CV (2005) Mechanisms of resistance of malaria parasites to antifolates. Pharmacol Rev 57: 117-145.

13. Noedl H, Se Y, Sriwichai S, Schaecher K, Teja-Isavadharm P, et al. (2010) Artemisinin resistance in Cambodia: a clinical trial designed to address an emerging problem in Southeast Asia. Clin Infect Dis 51: e82-89.

14. Woodrow CJ, Bustamante LY (2011) Mechanisms of artemisinin action and resistance: wider focus is needed. Trends Parasitol 27: 2-3

15. O'Brien C, Henrich PP, Passi N, Fidock DA (2011) Recent clinical and molecular insights into emerging artemisinin resistance in *Plasmodium falciparum*. Curr Opin Infect Dis 24: 570-577.

16. Zarocostas J (2011) WHO unveils plan to stop artemisinin resistance "dead in its tracks". BMJ 342: d211.

17. Lorca T, Castro A (2012) The Greatwall kinase: a new pathway in the control of the cell cycle. Oncogene doi: 10.1038/onc.2012.79. [Epub ahead of print].

18. Gantke T, Sriskantharajah S, Sadowski M, Ley SC (2012) IkappaB kinase regulation of the TPL-2/ERK MAPK pathway. Immunol Rev 246: 168-182.

19. Cai Z, Zhao Y, Zhao B (2012) Roles of Glycogen synthase kinase 3 in Alzheimer's disease. Curr Alzheimer Res 9(7):864-79.

20. Ward P, Equinet L, Packer J, Doerig C (2004) Protein kinases of the human malaria parasite *Plasmodium falciparum*: the kinome of a divergent eukaryote. BMC Genomics 5: 79.

21. Sharma A (2000) Protein tyrosine kinase activity in human malaria parasite *Plasmodium falciparum*. Indian J Exp Biol 38: 1222-1226.

22. Kato K, Sugi T, Iwanaga T (2012) Roles of Apicomplexan protein kinases at each life cycle stage. Parasitol Int 61: 224-234.

23. Lim DC, Cooke BM, Doerig C, Saeij JP (2012) *Toxoplasma* and *Plasmodium* protein kinases: roles in invasion and host cell remodelling. Int J Parasitol 42: 21-32.

24. Hora R, Bridges DJ, Craig A, Sharma A (2009) Erythrocytic casein kinase II regulates cytoadherence of *Plasmodium falciparum*-infected red blood cells. J Biol Chem 284: 6260-6269.

25. Holton S, Merckx A, Burgess D, Doerig C, Noble M, et al. (2003) Structures of P. falciparum PfPK5 test the CDK regulation paradigm and suggest mechanisms of small molecule inhibition. Structure 11: 1329-1337.

26. Solyakov L, Halbert J, Alam MM, Semblat JP, Dorin-Semblat D, et al. (2011) Global kinomic and phospho-proteomic analyses of the human malaria parasite *Plasmodium falciparum*. Nat Commun 2: 565.

27. Smilkstein M, Sriwilaijaroen N, Kelly JX, Wilairat P, Riscoe M (2004) Simple and inexpensive fluorescence-based technique for high-throughput antimalarial drug screening. Antimicrob Agents Chemother 48: 1803-1806.

28. Bennett TN, Paguio M, Gligorijevic B, Seudieu C, Kosar AD, et al. (2004) Novel, rapid, and inexpensive cell-based quantification of antimalarial drug efficacy. Antimicrob Agents Chemother 48: 1807-1810.

29. Harris CJ, Hill RD, Sheppard DW, Slater MJ, Stouten PF (2011) The design and application of target-focused compound libraries. Comb Chem High Throughput Screen 14: 521-531.

30. Menard R (2005) Medicine: knockout malaria vaccine? Nature 433: 113-114.

31. Green JL, Rees-Channer RR, Howell SA, Martin SR, Knuepfer E, et al. (2008) The motor complex of *Plasmodium falciparum*: phosphorylation by a calcium-dependent protein kinase. J Biol Chem 283: 30980-30989.

32. Kato N, Sakata T, Breton G, Le Roch KG, Nagle A, et al. (2008) Gene expression signatures and small-molecule compounds link a protein kinase to *Plasmodium falciparum motility*. Nat Chem Biol 4: 347-356.

33. Gilk SD, Gaskins E, Ward GE, Beckers CJ (2009) GAP45 phosphorylation controls assembly of the *Toxoplasma* myosin XIV complex. Eukaryot Cell 8: 190-196.

34. Pogacic V, Bullock AN, Fedorov O, Filippakopoulos P, Gasser C, et al. (2007) Structural analysis identifies imidazo[1,2-b]pyridazines as PIM kinase inhibitors with in vitro antileukemic activity. Cancer Res 67: 6916-6924.

35. Ghose AK, Herbertz T, Pippin DA, Salvino JM, Mallamo JP (2008) Knowledge based prediction of ligand binding modes and rational inhibitor design for kinase drug discovery. J Med Chem 51: 5149-5171.

36. Swinney DC, Anthony J (2011) How were new medicines discovered? Nat Rev Drug Discov 10: 507-519.

37. Cameron A, Read J, Tranter R, Winter VJ, Sessions RB, et al. (2004) Identification and activity of a series of azole-based compounds with lactate dehydrogenase-directed anti-malarial activity. J Biol Chem 279: 31429-31439.

38. Buchholz K, Putrianti ED, Rahlfs S, Schirmer RH, Becker K, et al. (2010) Molecular genetics evidence for the in vivo roles of the two major NADPH-dependent disulfide reductases in the malaria parasite. J Biol Chem 285: 37388-37395.

39. Harper JF, Harmon A (2005) Plants, symbiosis and parasites: a calcium signalling connection. Nat Rev Mol Cell Biol 6: 555-566.

40. Baum J, Richard D, Healer J, Rug M, Krnajski Z, et al. (2006) A conserved molecular motor drives cell invasion and gliding motility across malaria life cycle stages and other apicomplexan parasites. J Biol Chem 281: 5197-5208.

41. Baum J, Papenfuss AT, Baum B, Speed TP, Cowman AF (2006) Regulation of apicomplexan actin-based motility. Nat Rev Microbiol 4: 621-628.

42. Billker O, Lourido S, Sibley LD (2009) Calcium-dependent signaling and kinases in apicomplexan parasites. Cell Host Microbe 5: 612-622.

43. Wernimont AK, Artz JD, Finerty P, Jr., Lin YH, Amani M, et al. (2010) Structures of apicomplexan calcium-dependent protein kinases reveal mechanism of activation by calcium. Nat Struct Mol Biol 17: 596-601.

44. Murphy RC, Ojo KK, Larson ET, Castellanos-Gonzalez A, Perera BG, et al. (2010) Discovery of potent and selective inhibitors of calcium-dependent protein kinase 1 (CDPK1) from *C. parvum* and *T. gondii*. ACS Med Chem Lett 1: 331-335.

45. Larson ET, Ojo KK, Murphy RC, Johnson SM, Zhang Z, et al. (2012) Multiple determinants for selective inhibition of apicomplexan calcium-dependent protein kinase CDPK1. J Med Chem 55: 2803-2810.

46. Johnson SM, Murphy RC, Geiger JA, DeRocher AE, Zhang Z, et al. (2012) Development of *Toxoplasma gondii* calcium-dependent protein kinase 1 (TgCDPK1) inhibitors with potent anti-toxoplasma activity. J Med Chem 55: 2416-2426.

47. Lemercier G, Fernandez-Montalvan A, Shaw JP, Kugelstadt D, Bomke J, et al. (2009) Identification and characterization of novel small molecules as potent inhibitors of the plasmodial calcium-dependent protein kinase 1. Biochemistry 48: 6379-6389.

48. Billker O, Dechamps S, Tewari R, Wenig G, Franke-Fayard B, et al. (2004) Calcium and a calcium-dependent protein kinase regulate gamete formation and mosquito transmission in a malaria parasite. Cell 117: 503-514.

49. Dvorin JD, Martyn DC, Patel SD, Grimley JS, Collins CR, et al. (2010) A plant-like kinase in *Plasmodium falciparum* regulates parasite egress from erythrocytes. Science 328: 910-912.

50. Ishino T, Orito Y, Chinzei Y, Yuda M (2006) A calcium-dependent protein kinase regulates *Plasmodium* ookinete access to the midgut epithelial cell. Mol. Microbiol. 59: 1175-1184.

Acknowledgements

First of all, I would like to thank to Institut Pasteur Korea (IPK) that allowed me to do my PhD. My all work was done in the Institute using IPK resources. I also thank to Dr. Rita Song who supported me as a chairman of PhD committee in IPK. Prior to thank to the people who were directly involved in and helped for my PhD project, I'd like to thank to all my friends in the Center for Neglected Disease Drug Discovery (CND3). Especially, I want to thank to my close friends, Fernando, John, Jair, Miriam and Carol who struggled with lots of unexpected conditions when the lab was not set up stably.

I want to thank to all the people who directly helped for this project. My supervisor, Dr. Lucio Freitas-Junior gave me this nice project for my PhD, in August 2011. I really appreciate to him that he gave me a lot of support and advise during my PhD. Also, I thank to Dr. Min-Ho Choi who was my co-supervisor in Seoul National University and supported me during my PhD. Dr. Lawrence Ayong who is the team leader of Malaria group in IPK, he gave me his idea and spent time to discuss with me regarding this project. I especially want to thank to the external collaborators, Dr. Christian Doerig and Dr. Isabelle Lucet who tested my compounds in their recombinant *Plasmodium* kinases. I thank to John and Jair who were responsible for cytotoxicity test for Biofocus library and shared the data with me. I appreciate to Lawrence who let me use the image-based *T. gondii* proliferation assay. I also want to thank to Dr. Joohwan No who performed molecular docking analysis using my three compounds and taught me how to use MacPyMol. I also thank to Brazilian interns and Luis and Joana (Portuguese PhD students) who I met here in the center. There were many interns came and gone already, forgive me that I don't mention all your names here due to the limited space.

Lastly, I thank to my family who always supported me and cheered me up during my PhD. Especially to my husband, Jaeho, who took care of our little daughter alone whenever I had to work during weekends. I wouldn't have made this achievement without you! I also feel sorry and thank to my little daughter, Yubin. She didn't get her mom's full attention because her mom was very busy. I will promise to my husband and daughter that I would be better wife and mom for you from now.

감사합니다. Beijos! Love you all!

국문 초록

연구배경: 전 세계적으로 한 해 백만 명의 목숨을 앗아가는 말라리아는 약제내성으로 인해 쉽게 퇴치되지 않고 있어 새로운 항말라리아제 개발이 절실한 상태이다. 2004년 게놈 분석 프로젝트의 결과로 밝혀진 열원충의 키나아제는 약 100여개 존재하는데, 일차 구조가 eukaryotic protein kinase와는 매우 다른 orphan kinase이거나 semi orphan kinase로서 항말라리아제 개발의 좋은 표적이 될 수 있다. 본 연구에서는 열원충의 키나아제에 특이적인 저해제를 발굴함으로써 항말라리아제의 후보 물질을 탐구하고자 하였다.

연구방법: 열원충의 키나아제를 특이적으로 저해할 수 있는 물질을 발굴하기 위하여 여러 키나아제 저해재들로 구성된 4000개의 컴파운드 라이브러리를 두 종류의 열원충주 (wild type인 3D7과 약제 내성주 Dd2)에 처리하여 SYBR Green I assay를 이용하여 스크리닝하였다. 이후 fluorescence-based thermal shift assay (FSA)와 kinase assay를 이용하여, 일차 스크리닝으로부터 나온 hit들이 어떤 열원충의 키나아제를 표적하는지 탐구하였다. 또한, 그 hit을 열원충과 같은 Apixomplexa 문(門)에 속하는 톡소포자충 (*Toxoplasma gondii*)에 처리하여 표적 단백질을 증명하였다. 마지막으로 *in silico* 분자 모델링을 통하여 최종 hit이 표적하는 단백질에 어떻게 결합하는지 관찰하였다.

연구결과: 일차 스크리닝 결과 총 23개의 컴파운드가 1 μM 이내의 EC_{50}로 두 열원충주에 대하여 활성을 나타내었으며 이 컴파운드들은 4종류의 인간세포에는 거의 독성을 나타내지 않았다. Fluorescence-based thermal shift assay (FSA)와 kinase assay를 통해서 23개 컴파운드 중 3개가 *Plasmodium falciparum* calcium dependent protein kinase 1 (PfCDPK1)을 표적하는 것임을 확인하였다. 이 세개의 컴파운드를 톡소포자충에 처리하였을 때 기생충의 침범 과정을 특이적으로 저해한다는 사실을 확인하였고, CDPK1이 기생충의 운동성, 특히 침범에서 중요한 키나아제이므로 세 컴파운드가 CDPK1을 표적함을 간접적으로 증명해 준다. 또한, 알려진 CDPK1 구조를 이용하여 분자 모델링을 하였을 때, 세 컴파운드가 CDPK1의 active 사이트에 결합하는 모드가 전형적인 키나아제 저해제의 결합모드와 다르

다는 사실을 확인하였다.

결론: 이 연구에서 발굴한 총 23개의 컴파운드는 구조적으로 새로운 것일 뿐만 아니라, 인간 세포에는 독성을 나타내지 않은 채, wild type 말라리아 원충 및 약제 내성 충주에도 높은 활성을 나타내므로, 향후 새로운 항 말라리아제의 개발에 도움이 될 것으로 예상된다. 특히, PfCDPK1을 표적하는 세 물질의 발굴은 CDPK1을 표적으로 하는 새로운 항말라리아제를 디자인 하는데 도움을 줄 것으로 기대한다.

주요어 : 말라리아, 열원충, 항말라리아제, 키나아제, 키나아제 저해재, CDPK1
학 번 : 2009-31098